 CMES, vol.22, no.1, pp.77-89, 2007

Modeling of Degraded Composite Beam Due to Moisture Absorption For Wave Based Detection.

Shamsh Tabrez, Mira Mitra and S. Gopalakrishnan[1]

Abstract: In this paper, wave propagation is studied in degraded composite beam due to moisture absorption. The obtained wave responses are then used for diagnosis of the degraded zone. Moisture absorption causes an irreversible hygrothermal deterioration of the material. The change in temperature and moisture absorption changes the mechanical properties. Thus this affects the structure in dimensional stability as well as material degradation due to reduction in mechanical properties. Here, the composite beam is modeled as Timoshenko beam using wavelet based spectral finite element (WSFE) method. The WSFE technique is especially tailored for simulation of wave propagation. It involves Daubechies scaling function approximation in time and spectral finite element approach. The simulated wave responses are then used as surrogate experimental results to predict degradation using a measure called damage force indicator (DFI). Numerical experiments are presented for moisture absorbed composite beam due to modulated sinusoidal excitation. The responses are studied for different environmental conditions in term of relative humidity and at a temperature.

Keyword: Composite; moisture absorption; material degradation; damage detection; wave propagation; spectral finite element

1 Introduction

In the recent years there has been tremendous growth in composite technology as well as it's uses due to it's excellent strength to weight ratio, tailor-ability, thermal insulation to name few. These days it is extensively used in automobile and aerospace industries. Besides the advantages mentioned it has some inherent disadvantages too. Here, we will discuss about the degradation in material property due to moisture absorption. When composite material is exposed to humid atmosphere, many polymeric matrix composites absorb moisture by instantaneous surface absorption followed by diffusion through the matrix. Moisture will enter the interface of fiber and matrix due to the capillary action [Jihua and Maosheng (2004)]. The polymer matrix and the interface between the matrix and fiber can be degraded by hydrolysis reaction of unsaturated groups within the resin [Kootsooks and Mouritz (2004); Vera and Vazquez (2004)]. Debonding may occur at fiber/matrix interface [Imielinska and Guillaumat (2004)]. Composite material degradation occurs as cracks of the matrix material or/and fiber/matrix debonding, resulting from differential swelling of fiber and matrix. The weakening of bonding between fiber and matrix and softening of matrix material are also the reasons behind decrease in composite strength. In order to utilize the full potential of composite materials for the structural applications, the moisture content of composite material has to be well defined in advance. Few researchers have done experiments in standard laboratory conditions to establish the effects of moisture concentration on the tension modulus of composite material [Tsai and Hahn (1980)]. The hygrothermal deformation of an unidirectional composite is much higher in the transverse direction than in the longitudinal direction. Such difference in deformation in two directions induces residual stresses in composite laminates. This is because the multi directionality of fiber orientation resists free deformations. Also, the change in temperature and moisture absorp-

[1] Department of Aerospace Engineering, Indian Institute of Science, Bangalore, India 560012 Corresponding author E-mail: krishnan@aero.iisc.ernet.in Fax:+91-80-23600134

tion changes the mechanical properties. This affects the structure in dimensional stability as well as material degradation due to reduction in mechanical properties. The physical effect of moisture absorption is the reduction in glass transition temperature T_g of the resin. At room temperature, the performance of resin may not change with reduction in T_g but at elevated temperature properties are severely affected.

With the composite material getting degraded after moisture absorption, *i.e* the tension modulus first slightly increases with relative humidity (RH) up to 50 percent of RH and then decreases with further increases in RH. Thus, stiffness of the structure varies with RH. This reduction in stiffness affect the performance of the structure. This problem is very important when composite is used for fabrication of aircraft structures. Structural design is primarily guided by stiffness due to the aeroelastic phenomenon. Presently, this degradation in stiffness in due course of time is taken care by over design of structure, which results in heavier components. This problem of over design can be tackled by periodic structural health monitoring to check the stiffness of the structure. In this paper we use wavelet based spectral finite element to capture the effects of material degradation on wave response. Moisture absorption and hence the variation in tension modulus of composite material is very critically dependent on the atmosphere on which the composite material is subjected to, and hence, the laboratory test of coupon alone will not not be sufficient for the health monitoring of actual composite structure. Hence, one needs to resort to some kind of non-destructive evaluation (NDE) techniques.

In this paper, wave based technique is used for detection of degraded zone in moisture absorbed beam. A proper understanding of the effects of such material degradation on the wave propagation characteristics is required prior to their application to damage detections. Here, first the moisture absorbed composite beam is modeled as Timoshenko beam with three degrees of freedom (dofs) namely, axial, transverse and rotation. The modeling of composite structures for wave propagation analysis has been presented by Murthy, Gopalakrishnan, and Nair (2007) and Han, Liu, and Li (2004). In the present paper, the modeling is done using wavelet based spectral finite element (WSFE) method [Mitra and Gopalakrishnan (2006a)] which is specially suited for wave propagation analysis. In WSFE, the governing partial differential equations are reduced to ODEs using compactly supported Daubechies scaling function for time approximation. These ODEs are solved exactly to derive the shape functions which gives the elemental dynamic stiffness matrix. The elemental matrix can be assembled similar to conventional finite element(FE) approach to model more complex structures. The method is computationally very efficient as compared to conventional finite element (FE) method, particulary for wave problems where the later method proves to be computationally prohibitive. In addition, unlike the prevalent Fourier transform based spectral finite element (FSFE) method, WSFE can accurately model finite length structures.

In wave propagation analysis, any impedance mismatch such as presence of boundary, defects or change in stiffness results in additional waves due to reflection. By capturing these additional reflections, one can identify the presence of damage/discontinuty. Verbis, Tsinopoulos, and Polyzos (2002), Smojver and Soric (2006) and Han, Ingber, and Schreyer (2006) have reported wave propagation in damaged composite structures. However, when the change in stiffness or defect size is very small, the change in velocity is very small and hence, the amplitude of these reflected wave will be very small and in general not interpretable visually from the response plot. For these circumstances, damage force indicator (DFI) [Schulz, Naser, Pai., and Chung (1998)] appears as a helpful measure. In brief, DFI is a force measure, which calculates the difference between the damaged and undamaged responses multiplied with the stiffness matrix of the undamaged structure. The value of DFI is maximum between the two nodes where the damage exits. Apart from this, the value of the DFI is a relative indicator of the extent of damage. References [Kumar, Mahapatra, and Gopalakrishnan (2004); Nag, Mahapatra, and Gopalakrish-

nan (2002)] explain the derivation of DFI in frequency domain in the context of FSFE modeling. In the present work, WSFE is used to model the degraded composite beam. As mentioned earlier, this numerical technique can easily model finite length waveguide and thus accurately simulate the wave response in time domain unlike FSFE. Here, DFI is calculated from the time domain responses. The method is described in detail in the later part of the paper.

The paper is organized as follows. In section 2, the wavelet transform and the spectral finite element formulation is explained for a composite Timoshenko beam with axial, transverse and rotational degrees of freedom. The next section deals with the derivation of damage force indicator, followed with a section on modeling of moisture absorbed degraded composite beam. Section 5 is on numerical experiments performed. Here, first wave propagation in moisture absorbed composite beam is studied for different extent of moisture absorption and locations of the degraded region. Next, these simulated responses are used as a replacement for experimental results to inversely detect the position and extend of degradation using damage force indicator. At the end conclusions are discussed.

2 Mathematical Modeling

2.1 Daubechies Compactly Supported Wavelets

In this section, a concise review of orthogonal basis of Daubechies wavelets [Daubechis (1992)] is provided. Wavelets, $\psi_{j,k}(t)$ forms compactly supported orthonormal basis for $\mathbf{L^2(R)}$. The wavelets and associated scaling functions $\varphi_{j,k}(t)$ are obtained by translation and dilation of single functions $\psi(t)$ and $\varphi(t)$ respectively.

$$\psi_{j,k}(t) = 2^{j/2}\psi(2^j t - k), \qquad j,k \in \mathbf{Z} \tag{1}$$

$$\varphi_{j,k}(t) = 2^{j/2}\varphi(2^j t - k), \qquad j,k \in \mathbf{Z} \tag{2}$$

The scaling functions $\varphi(t)$ are derived from the dilation or scaling equation,

$$\varphi(t) = \sum_k a_k \varphi(2t-k) \tag{3}$$

and the wavelet function $\psi(t)$ is obtained as

$$\psi(t) = \sum_k (-1)^k a_{1-k}\varphi(2t-k) \tag{4}$$

a_k are the filter coefficients and they are fixed for specific wavelet or scaling function basis. For compactly supported wavelets only a finite number of a_k are nonzero. The filter coefficients a_k are derived by imposing certain constraints on the scaling functions.

Let $P_j(f)(t)$ be the approximation of a function $f(t)$ in $\mathbf{L^2(R)}$ using $\varphi_{j,k}(t)$ as basis, at a certain level (resolution) j, then

$$P_j(f)(t) = \sum_k c_{j,k}\varphi_{j,k}(t), \qquad k \in \mathbf{Z} \tag{5}$$

2.2 Reduction of wave equations to ODEs

The governing differential wave equations for composite Timoshenko beam are obtained from those derived by Mitra and Gopalakrishnan (2006b) for higher order composite beam.

$$I_0\frac{\partial^2 u}{\partial t^2} - I_1\frac{\partial^2 \phi}{\partial t^2} - A_{11}\frac{\partial^2 u}{\partial x^2} + B_{11}\frac{\partial^2 \phi}{\partial x^2} = 0 \tag{6}$$

$$I_0\frac{\partial^2 w}{\partial t^2} - A_{55}\left(\frac{\partial^2 w}{\partial x^2} - \frac{\partial \phi}{\partial x}\right) = 0 \tag{7}$$

$$I_2\frac{\partial^2 \phi}{\partial t^2} - I_1\frac{\partial^2 u}{\partial t^2} - A_{55}\left(\frac{\partial w}{\partial x} - \phi\right) + B_{11}\frac{\partial^2 u}{\partial x^2} \tag{8}$$

$$- D_{11}\frac{\partial^2 \phi}{\partial x^2} = 0 \tag{9}$$

$u(x,t)$, $w(x,t)$ and $\phi(x,t)$ are the axial, flexural and shear displacements respectively (see Fig. 1(a)). The stiffness coefficients are functions of ply properties, orientations etc and are obtained by integrating over the beam cross section as

$$[A_{ij},\, B_{ij},\, D_{ij}] = \sum \int_{z_i}^{z_{i+1}} \overline{Q}_{ij}[1,\, z,\, z^2]bdz \tag{10}$$

where, $\overline{Q}_{ij}$ are the transformed stiffness coefficients of each ply. z_i and z_{i+1} are the thickness coordinate of the i$^{\text{th}}$ layer and b is the corresponding width. Similarly, the inertial constants are obtained as

$$[I_0,\, I_1,\, I_2] = \sum \int_{z_i}^{z_{i+1}} \rho[1,\, z,\, z^2]bdz \tag{11}$$

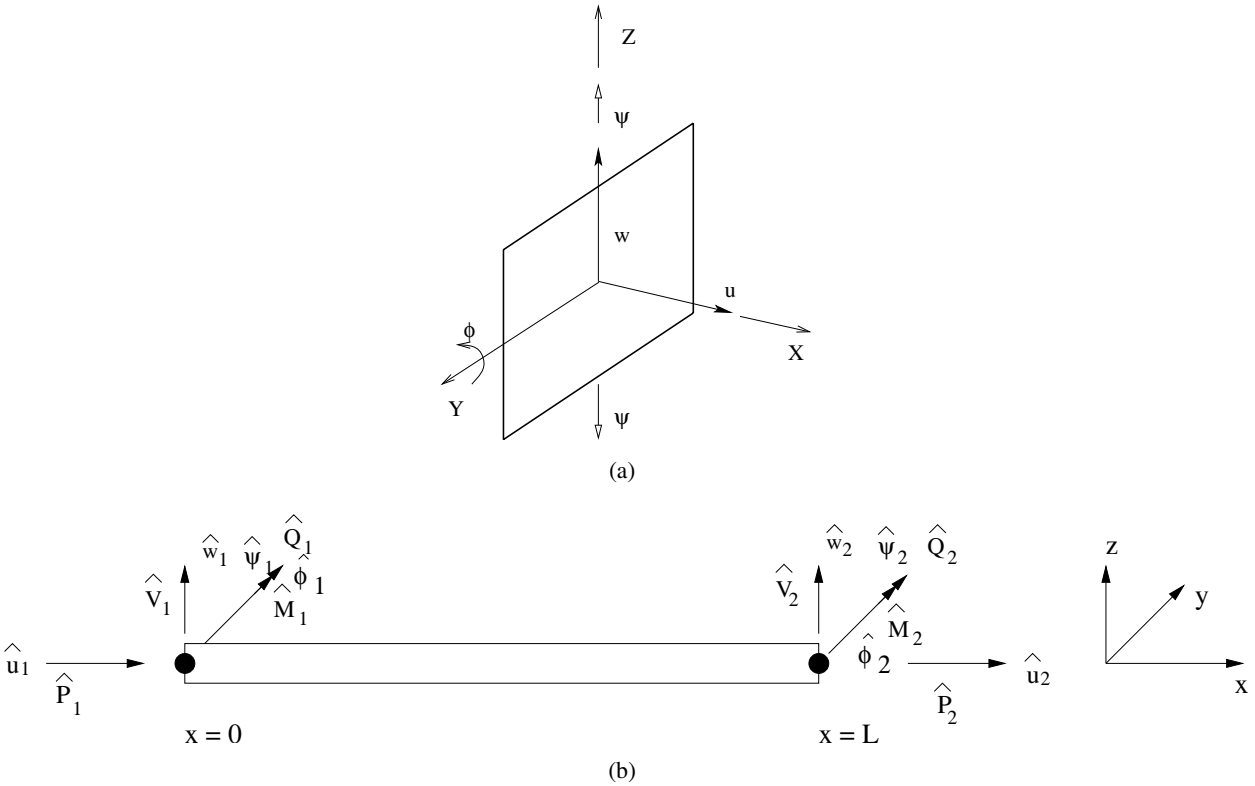

Figure 1: (a) Beam cross section and the displacements (b) Composite beam element with nodal displacements and forces

where, ρ is the mass density. The force boundary conditions associated with the governing differential equations are

$$A_{11}\frac{\partial u}{\partial x} - B_{11}\frac{\partial \phi}{\partial x} = P \tag{12}$$

$$A_{55}\frac{\partial w}{\partial x} - A_{55}\phi = V \tag{13}$$

$$-B_{11}\frac{\partial u}{\partial x} + D_{11}\frac{\partial \phi}{\partial x} = M \tag{14}$$

where, $P(x,t)$, $V(x,t)$ and $M(x,t)$ are the axial, transverse forces and moment respectively.

The first step of formulation of WSFE is the reduction of the governing differential wave equations (Eqns 6 to 9) to ODEs using Daubechies scaling functions for approximation in time. Let $u(x,t)$ be discretized at n points in the time window $[0\, t_f]$. Let $\tau = 0,\ 1, \ldots,\ n-1$ be the sampling points, then

$$t = \triangle t\, \tau \tag{15}$$

where, $\triangle t$ is the time interval between two sampling points. The function $u(x,t)$ can be approximated by scaling function $\varphi(\tau)$ at an arbitrary scale as

$$u(x,t) = u(x,\tau) = \sum_k u_k(x)\varphi(\tau - k), \quad k \in \mathbf{Z} \tag{16}$$

where, $u_k(x)$ (referred as u_k hereafter) are the approximation coefficient at a certain spatial dimension x. The other displacements $w(x,t)$, $\phi(x,t)$ can be transformed similarly and Eqn. 6 can be written as

$$\frac{I_0}{\triangle t^2}\sum_k u_k \varphi''(\tau - k) - \frac{I_1}{\triangle t^2}\sum_k \phi_k \varphi''(\tau - k) + \sum_k \left(-A_{11}\frac{d^2 u_k}{dx^2} + B_{11}\frac{d^2 \phi_k}{dx^2}\right)\varphi(\tau - k) = 0 \tag{17}$$

Taking inner product on both sides of Eqns. 17 with the translates of scaling functions $\varphi(\tau - j)$, where $j = 0,\ 1, \ldots, n-1$ and using their orthogo-

nal properties, we get n simultaneous ODEs as,

$$\frac{1}{\triangle t^2}\sum_{k=j-N+2}^{j+N-2}\Omega^2_{j-k}(I_0u_k - I_1\phi_k) - A_{11}\frac{d^2u_j}{dx^2} + B_{11}\frac{d^2\phi_j}{dx^2} = 0 \quad j = 0,\ 1,\ldots,n-1 \quad (18)$$

where, N is the order of the Daubechies wavelet and Ω^2_{j-k} are the connection coefficients defined as

$$\Omega^2_{j-k} = \int \varphi''(\tau-k)\varphi(\tau-j)d\tau \quad (19)$$

Similarly, for first order derivative Ω^1_{j-k} are defined as

$$\Omega^1_{j-k} = \int \varphi'(\tau-k)\varphi(\tau-j)d\tau \quad (20)$$

For compactly supported wavelets, $\Omega^1_{j-k},\ \Omega^2_{j-k}$ are nonzero only in the interval $k = j-N+2$ to $k = j+N-2$. The details for evaluation of connection coefficients for different orders of derivative is given by [Beylkin (1992)].

It can be observed from the ODEs given by Eqn. 18 that certain coefficients u_j near the vicinity of the boundaries ($j = 0$ and $j = n-1$) lie outside the time window $[0\ t_f]$ defined by $j = 0,\ 1,\ldots,n-1$. This coefficients must be treated properly for finite domain analysis. Several approaches like capacitance matrix methods, penalty function methods for treating boundaries are reported in the literature. In this paper, a wavelet based extrapolation scheme [Williams and Amaratunga (1997)] is implemented for solution of boundary value problems. This approach allows treatment of finite length data and uses polynomial to extrapolate the coefficients lying outside the finite domain either from interior coefficients or initial/boundary values. The method is particularly suitable for approximation in time for the ease to impose initial values. The above method converts the ODEs given by Eqns 18 to a set of coupled ODEs given as

$$\left[\Gamma^1\right]^2(I_0\{u_j\} - I_1\{\phi_j\}) - A_{11}\left\{\frac{d^2u_j}{dx^2}\right\} + B_{11}\left\{\frac{d^2\phi_j}{dx^2}\right\} = 0 \quad (21)$$

where Γ^1 is the first order connection coefficient matrix obtained after using the wavelet extrapolation technique. It should be mentioned here that though the connection coefficients matrix, Γ^2, for second order derivative can be obtained independently, here it is written as $[\Gamma^1]^2$ as it helps to impose the initial conditions [Mitra and Gopalakrishnan (2005)]. These coupled ODEs are similarly decoupled using eigenvalue analysis

$$\Gamma^1 = \Phi\Pi\Phi^{-1} \quad (22)$$

where, Π is the diagonal eigenvalue matrix and Φ is the eigenvectors matrix of Γ^1. Let the eigenvalues be $i\gamma_j$, then the decoupled ODEs corresponding to Eqns. 21 are

$$-I_0\gamma_j^2\widehat{u}_j + I_1\gamma_j^2\widehat{\phi}_j - A_{11}\frac{d^2\widehat{u}_j}{dx^2} + B_{11}\frac{d^2\widehat{\phi}_j}{dx^2} = 0 \quad j = 0,\ 1,\ldots,n-1 \quad (23)$$

where, $\widehat{u}_j$ and similarly other transformed displacements are

$$\widehat{u}_j = \Phi^{-1}u_j \quad (24)$$

Following exactly the similar steps, the final transformed form of the Eqns. 7 and 9 are

$$-I_0\gamma_j^2\widehat{w}_j - A_{55}\left(\frac{d^2\widehat{w}_j}{dx^2} - \frac{d\widehat{\phi}_j}{dx}\right) = 0 \quad (25)$$

$$-I_2\gamma_j^2\widehat{\phi}_j - I_1\gamma_j^2\widehat{u}_j - A_{55}\left(\frac{d\widehat{w}_j}{dx} - \widehat{\phi}_j\right) + B_{11}\frac{d^2\widehat{u}_j}{dx^2} - D_{11}\frac{d^2\widehat{\phi}_j}{dx^2} = 0 \quad (26)$$

(27)

Similarly, the transformed form of the force boundary conditions given by Eqns. 12 to 14 are

$$A_{11}\frac{d\widehat{u}_j}{dx} - B_{11}\frac{d\widehat{\phi}_j}{dx} = P_j \quad (28)$$

$$A_{55}\frac{d\widehat{w_j}}{dx} - A_{55}\widehat{\phi}_j = V_j \quad (29)$$

$$-B_{11}\frac{d\widehat{u}_j}{dx} + D_{11}\frac{d\widehat{\phi}_j}{dx} = M_j \quad j = 0,\ 1,\ldots,n-1 \quad (30)$$

where, P_j and similarly V_j, M_j are the transformed $P(x,t)$ and $V(x,t)$, $M(x,t)$ respectively.

2.3 Spectral finite element formulation

The degrees of freedom associated with the element formulation is shown in Fig. 1(b). The element has 3 degrees of freedom per node, which are $\widehat{u}_j$, $\widehat{w}_j$ and $\widehat{\phi}_j$. From the previous sections, we get a set of ODEs (Eqns. 23, 25 and 26) for composite beam with axial, transverse and shear modes, in a transformed wavelet domain. These equations are required to be solved for $\widehat{u}_j$, $\widehat{w}_j, \widehat{\phi}_j$ and the actual solutions $u(x,t)$, $w(x,t)$, $\phi(x,t)$ are obtained using inverse wavelet transform. For finite length data, the wavelet transform and its inverse can be obtained using a transformation matrix [Williams and Amaratunga (1994)].

It can be seen that the transformed ODEs have a form which is similar to that in FSFE [Doyle (1999)] and thus, WSFE can be formulated following the same method as for FSFE formulation. In this section, the subscript j is dropped hereafter for simplified notations and all the following equations are valid for $j = 0,\ 1,\ \ldots,\ n-1$.

The exact interpolating functions for an element of length L, obtained by solving Eqns. 23, 25 to 26 respectively, can be written as,

$$\left\{\widehat{u}(x),\ \widehat{w}(x),\ \widehat{\phi}(x)\right\}^T = [\mathbf{R}][\mathbf{\Theta}]\{\mathbf{a}\} \tag{31}$$

where, $[\mathbf{\Theta}]$ is a diagonal matrix with the diagonal terms $[e^{-k_1 x},\ e^{-k_1(L-x)},\ e^{-k_2 x},\ e^{-k_2(L-x)},\ e^{-k_3 x},\ e^{-k_3(L-x)}]$ and $[\mathbf{R}]$ is a 3×6 amplitude ratio matrix for each set of $k_1,\ k_2$ and k_3.

$$[\mathbf{R}] = \begin{bmatrix} R_{11} & \ldots\ \ldots & R_{16} \\ R_{21} & \ldots\ \ldots & R_{26} \\ R_{31} & \ldots\ \ldots & R_{36} \end{bmatrix} \tag{32}$$

$k_1,\ k_2$ and k_3 are obtained by substituting Eqn. 31 in Eqns 23, 25 and 26 and solving the characteristic equation. The characteristic equation is obtained by equating the determinant of the 3×3 companion matrix to zero. The corresponding $[\mathbf{R}]$ is obtained using singular value decomposition of the matrix. This method of determining wavenumbers and corresponding amplitude ratios was developed to formulate FSFE for graded beam with Poisson's contraction by Chakraborty and Gopalakrishnan (2004). $k_1,\ k_2$ and k_3 corresponds to the three modes *i.e* axial, transverse and shear respectively and as explained in reference [Mitra and Gopalakrishnan (2005)], these are the wavenumbers but only up to a certain fraction of Nyquist frequency.

Here, $\{\mathbf{a}\} = \{\text{A, B, C, D, E, F}\}$ are the unknown wave coefficients to be determined from transformed nodal displacements $\widehat{\mathbf{u}}^{\mathbf{e}}$, where $\widehat{\mathbf{u}}^{\mathbf{e}} = \{\widehat{u}_1\ \widehat{w}_1\ \widehat{\phi}_1\ \ \widehat{u}_2\ \widehat{w}_2\ \widehat{\phi}_2\}$ and $\widehat{u}_1 \equiv \widehat{u}(0)$, $\widehat{w}_1 \equiv \widehat{w}(0)$, $\widehat{\phi}_1 \equiv \widehat{\phi}(0)$ and $\widehat{u}_2 \equiv \widehat{u}(L)$, $\widehat{w}_2 \equiv \widehat{w}(L)$, $\widehat{\phi}_2 \equiv \widehat{\phi}(L)$, (see Fig. 1(b) for the details of degree of freedom the element can support). Thus we can relate the nodal displacements and unknown coefficients as

$$\widehat{\mathbf{u}}^{\mathbf{e}} = [\mathbf{B}]\{\mathbf{a}\} \tag{33}$$

From the forced boundary conditions, (Eqns. 28 to 30), nodal forces and unknown coefficients can be related as

$$\widehat{\mathbf{F}}^{\mathbf{e}} = [\mathbf{C}]\{\mathbf{a}\} \tag{34}$$

where, $\widehat{\mathbf{F}}^{\mathbf{e}} = \{\widehat{P}_1\ \widehat{V}_1\ \widehat{M}_1\ \widehat{P}_2\ \widehat{V}_2\ \widehat{M}_2\}$ and $\widehat{P}_1 \equiv \widehat{P}(0)$, $\widehat{V}_1 \equiv \widehat{V}(0)$, $\widehat{M}_1 \equiv \widehat{M}(0)$ and $\widehat{P}_2 \equiv -\widehat{P}(L)$, $\widehat{V}_2 \equiv -\widehat{V}(L)$, $\widehat{M}_2 \equiv -\widehat{M}(L)$ (see Fig. 1(b)). From Eqns. 33 and 34 we can obtain a relation between transformed nodal forces and displacements similar to conventional FE

$$\widehat{\mathbf{F}}^{\mathbf{e}} = [\mathbf{C}][\mathbf{B}]^{-1}\widehat{\mathbf{u}}^{\mathbf{e}} = \widehat{\mathbf{K}}^{\mathbf{e}}\widehat{\mathbf{u}}^{\mathbf{e}} \tag{35}$$

where $\widehat{\mathbf{K}}^{\mathbf{e}}$ is the exact elemental dynamic stiffness matrix. After the constants $\{\mathbf{a}\}$ are known from the above equations, they can substituted back to Eqn. 31 to obtain the transformed displacements $\widehat{u},\ \widehat{w},\ \widehat{\phi}$ at any given x.

3 Identification of Degraded Material Zone Using Damage Force Indicator Method

The concept of damage force has been used by Schulz, Naser, Pai., and Chung (1998) to derive a damage indicator, which can detect the elements having flaws in a finite element model. Kumar, Mahapatra, and Gopalakrishnan (2004); Nag, Mahapatra, and Gopalakrishnan (2002) used this technique effectively to identify delamination and transverse crack in composite beam using FSFE model. Here, DFI was calculated in the frequency domain for the FSFE model. In brief,

DFI is a force measure which calculates the difference between the damaged and undamaged responses multiplied with the stiffness matrix of the undamaged structure. In the absence of the experimental data, simulated responses of both the healthy and damage structure models are used to compute the damage force indicator, which actually demonstrate a simulated sequence of identification procedure in real life. In this work, the moisture absorbed degraded beam is modeled using WSFE method discussed elaborately in the previous section. The global dynamic stiffness matrix of the healthy structure $\hat{K}_h^G$ is obtained by assembling the element dynamic stiffness matrix $\hat{K}_e$ given in Eqn. 35. The damage force vector at each sampling point; is given as

$$\begin{aligned} \Delta\hat{F} &= \hat{K}_h^G(\hat{u}_d - \hat{u}_h); \\ &= \hat{K}_h^G\hat{u}_d - \hat{K}_h^G\hat{u}_h \end{aligned} \tag{36}$$

where, subscripts d and h refer to degraded and healthy structures respectively. The basic procedure is as follows; first of all the rotational velocity and transverse velocity is measured experimentally at different locations. Then these measured velocities v are transformed from time domain to wavelet domain $\hat{v}$ using Daubechies scaling function approximation. After this transformation to wavelet domain the velocity is converted to displacement at each sampling point. The relation between $\hat{v}$ and $\hat{u}$ is given as, $\hat{v}_j = -\iota\gamma_j\hat{u}_j$. This experimentally measured and transformed displacement vectors when multiplied by the stiffness matrix of healthy structure gives the force at each corresponding nodes at all sampling points. The summation of the square of real part of the force vector for all the sampling point gives the DFI. From Eqn. 36, it is evident that DFI measures the change in state of stress between damaged and undamaged beams. Hence, $\Delta\widehat{F}$ will be zero if there is no damage (*i.e.* there is no change in state of stress) and will have non-zero value at that nodes where there is damage (*i.e.* there is change in state of stress due to damage). Magnitude of these non zero entries depends on the extend of damage.

4 Modeling of Degradation

4.1 Moisture Absorption

When composite material is exposed to humid atmosphere, many polymeric matrix composites absorbs moisture by instantaneous surface absorption followed by diffusion through the matrix. Moisture will enter the interface of fiber and matrix due to the capillary action [Jihua and Maosheng (2004)]. The polymer matrix and the interface between the matrix and fiber can be degraded by hydrolysis reaction of unsaturated groups within the resin [Kootsooks and Mouritz (2004); Vera and Vazquez (2004)]. Debonding may occur at fiber/matrix interface [Imielinska and Guillaumat (2004)]. Composite material degradation occurs as cracks of the matrix material or/and fiber/matrix debonding, resulting from differential swelling of fiber and matrix. The weakening of bonding between fiber and matrix and softening of matrix material are also the reasons behind decrease in composite strength. Few researchers have done experiments in standard laboratory conditions to establish the affect of moisture concentration in the tension modulus of composite material [Tsai and Hahn (1980)].

The moisture concentration increases with time and reaches the saturation level after some prescribed time. The maximum moisture content depends on the environment. In humid air it is a function of relative humidity. It has been found that maximum moisture content, C_m can be related to the relative humidity ϕ by the expression [Shen and Springer (1976)].

$$C_m = a\phi^b \tag{37}$$

where, a and b are constants which depend on material. The value of these constants can be obtained by fitting the line through the data points. Table 1 gives the values of a and b obtained by various researchers. It has been found that maximum moisture content is insensitive to the ambient temperature but depends on the relative humidity (RH) of the environment [Shen and Springer (1976)]. This is evident from Eqn. 37.

Figs. 2(a), (b) and (c), give the variation of Young's modulus E_x, E_y and E_z respectively in

Table 1: Values of a and b (used in Eqn. 37) for AS/3501

Investigator	a	b
Loos and Springer (1979)	0.019	1
DeIasi and Whiteside (1978)	0.0186	$1.6, \phi < 60$ % RH
-	-	$1.9, \phi > 60$ % RH
Whitney and Browing (1978)	0.016	1.1

composite with moisture concentration C, which is reproduced from reference [Tsai and Hahn (1980)]. These curves can be approximated as a higher order polynomial in moisture concentration. These approximations are given in the following equations for different temperature. This polynomial model is fed directly to the WSFE code for modeling and detection purpose. For temperature T = 366 K,

$$E_X = 16.344C^6 - 66.161C^5 + 92.479C^4 - 57.29C^3 + 13.769C^2 - 81.049C + 134.39 \quad (38)$$

$$E_Y = 4.5804C^6 - 20.11C^5 + 32.943C^4 - 24.297C^3 + 7.7994C^2 - 1.8376C + 9.6732 \quad (39)$$

$$E_Z = 1.2694C^6 - 6.2108C^5 + 11.629C^4 - 10.281C^3 + 4.129C^2 - 0.4398C + 6.0866 \quad (40)$$

For Temperature, T = 394K;

$$E_X = 16.344C^6 - 66.161C^5 + 92.479C^4 - 57.29C^3 + 13.769C^2 - 81.049C + 134.39 \quad (41)$$

$$E_Y = -5.8703C^4 + 11.744C^3 - 5.3871C^2 - 2.3500C + 7.7277 \quad (42)$$

$$E_Z = -0.7275C^4 + 1.8871C^3 - 1.6856C^2 - 0.3426C + 5.5415 \quad (43)$$

In this work, the degradation of composite due to moisture absorption is modeled with appropriate modulus as given by Eqn. 38 to 43 and location of this degraded zone is assumed at 0.25 m from the fixed end of the cantilever beam of 0.75 m total length. The length of this degradation zone is assumed to be 0.025 m. The schematic diagram of degraded beam is shown in Fig. 3.

5 Numerical Experiments

In this section, numerical examples are presented for a degraded (moisture absorbed) composite (AS/3501) cantilever beam. As said earlier, first the effects of degradation on the wave propagation are studied for different extents of degradation and location. Next, these simulated responses are used as surrogate experimental results to predict the damage inversely using damage force indicator.

5.1 Wave propagation analysis

The beam used for numerical experiments has a length, L = 0.75 m , width, b = 0.05 m, number of ply, n = 4 and ply thickness, t = 0.0013 m. The material properties are as follows, the Young modulus (E) is a function of moisture absorption and is given in Eqn. 38 to 43. In absence of data available for the variation of G with moisture absorption it is assumed to be constant and it's value is taken as, $G_{12} = G_{13} = 6.13$ GPa; $G_{23} = 4.80$ GPa; $\nu_{12} = 0.42$; mass density $= 1449$ kg/m^3; The Daubecheis scaling function used in these examples has an order of N $= 22$ and the sampling rate is Δt $= 1\mu$s. To calculate the moisture concentration, Eqn. 37 is used, where a = 0.0018 and b = 1 [Loos and Springer (1979)].

A sinusoidal pulse modulated at 37.6 kHz as shown in Fig. 4 is used as input signal. The modulated pulse contain maximum energy within a very small frequency band and peak energy will be at the frequency at which it is modulated. It is used extensively in experimental investigations as well as computational simulations for wave based diagnostics.

Fig. 5 shows the tip transverse velocity in beam due to modulated load applied at tip in transverse direction. The degraded region is at 0.25 m from the fixed end and is modeled with single WSFE. The responses are plotted for different values of relative humidity (RH) from 0 to 80 percent in the step of 20 percent. Fig. 6 gives the exploded

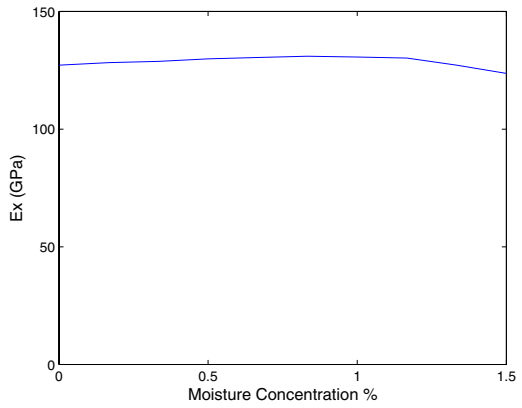

(a)

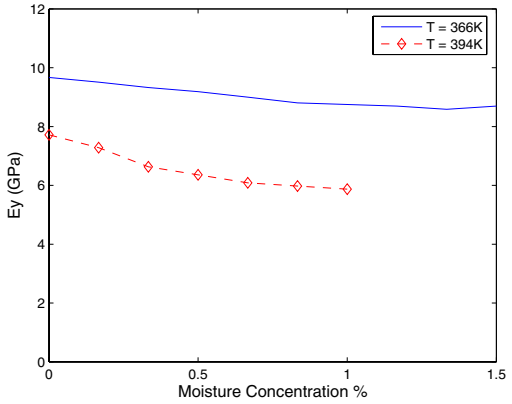

(b)

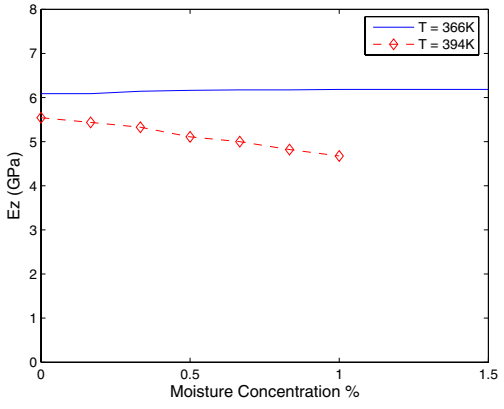

(c)

Figure 2: Variation of modulus (a) E_X, (b) E_y and (c) E_z with moisture concentration, Temp = 394K, 366K Tsai and Hahn (1980).

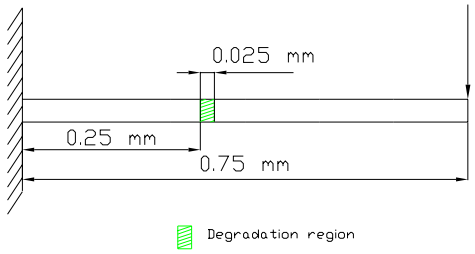

Figure 3: Schematic model of degraded composite beam

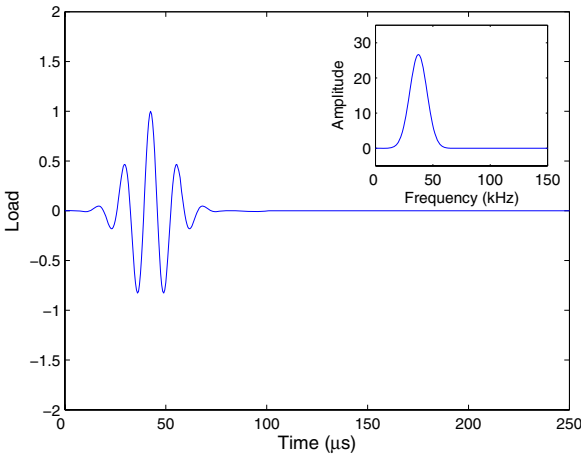

Figure 4: Modulated sinusoidal pulse at 37.6 kHz in time and frequency (inset) domains.

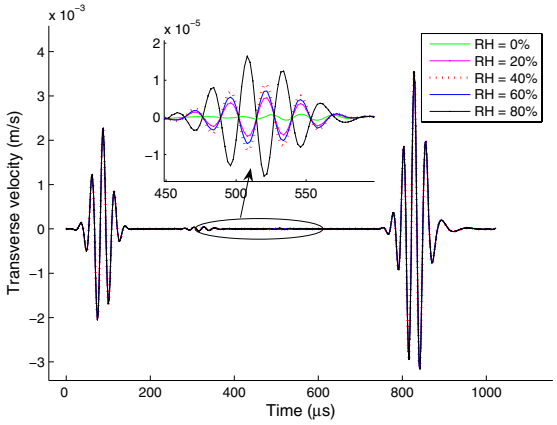

Figure 5: Transverse tip velocity in beam due to tip modulated load. for a temperature of 394 K

view of the reflection from the degraded zone. On careful observation from Fig. 6 it is found that the magnitude of response is increasing from 0 percent RH to 40 percent RH, subsequently it is decreasing and at 80 percent RH it's phase get changed. To investigate further, the response is further plotted as shown in Fig. 7 at smaller steps of increment in the percent of RH. Again on careful observation from Fig. 7 it is found that the magnitude of response is increasing from 0 percent RH to 50 percent RH and subsequently is decreasing and at magnitude corresponding to 30 percent RH and 60 percent RH, the responses are nearly same, which means that stiffness at these two values of RH is nearly same. When RH is increased from 70 percent, the phase get altered, which is in accordance with the variation in tension modulus E_X, which first increase up to 50 percent RH and then it decreases. After 70 percent RH, response decreases rapidly. Here, WSFE captures these variations in modulus effectively.

Finally, numerical experiments are performed using the measured transverse velocity responses to detect the presence of degraded zone. Fig. 8, shows the transverse velocity measured at the tip of of the degraded beam due to the modulated pulse load shown in Fig. 4 applied at tip in transverse direction. The response are plotted for different positions of degraded zone assumed, namely 0.125, 0.175, 0.250 m from the fixed end. The extent of degradation is at RH = 50%. It can be seen from Fig. 8 that time of arrival of the reflected wave shifts with the shift in the position of the degraded zone and this is as expected. The position of damage can be also be predicted from the time of arrival of the reflected wave. This can be done by multiplying the wave velocity known from dispersion relation with the time of arrival. This gives twice the distance of the damage from the point of application of load. However, in this case, since the extent of stiffness reduction is very small, the reflected waves are not visible in the response unless magnified as done in Fig. 8. Thus, for detection of such minute change in stiffness, a force measure called damage force indicator is used to detect the location and extend of damage. The efficiency of DFI in predicting the position

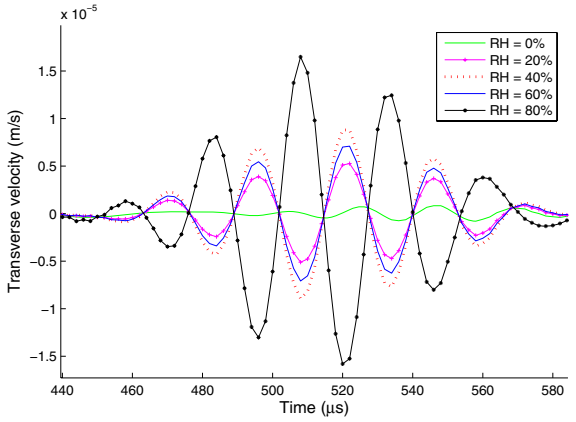

Figure 6: Transverse tip velocity in beam due to tip modulated load.

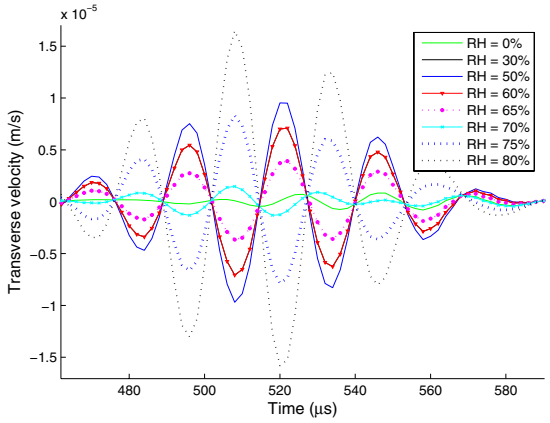

Figure 7: Transverse tip velocity in beam due to tip modulated load.

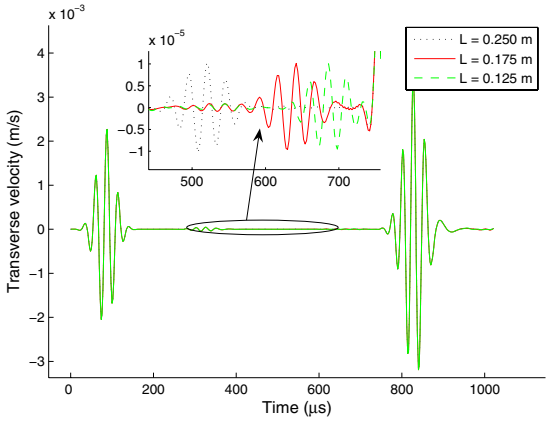

Figure 8: Response of degraded composite beam with degraded zone at various location.

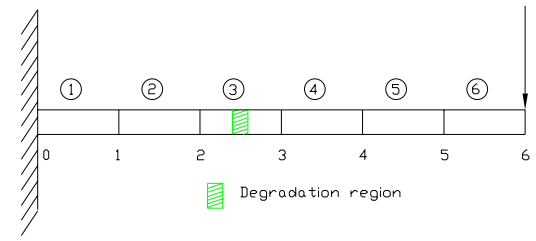

(a)

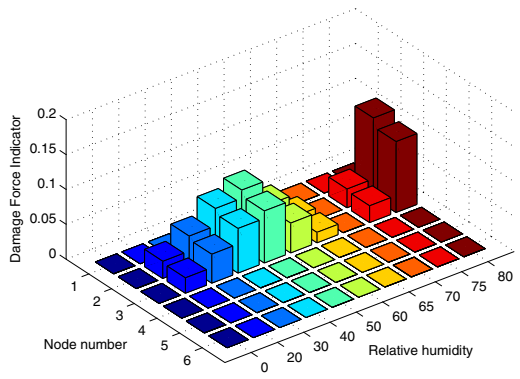

(b)

Figure 9: (a) Schematic of beam for 6 elements and (b) Damage force indicator for 6 elements.

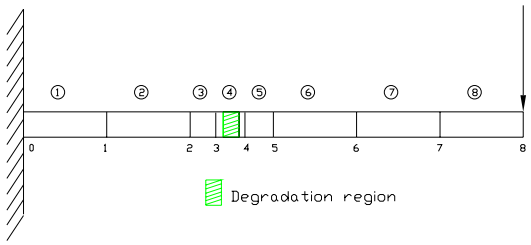

(a)

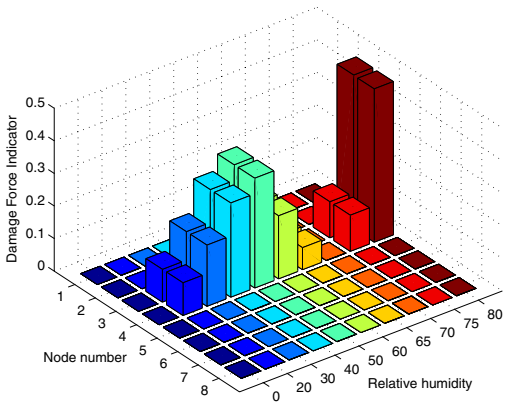

(b)

Figure 10: (a) Schematic of beam for 8 elements and (b) Damaged force indicator for 8 elements.

and extend of damage is emphasized through numerical examples in the next subsection.

5.2 Identification of Degraded Zone Using Damage Force Indicator

As mentioned earlier, DFI is a damage measure based on force residue that locates the position of damage and also predict the extent of damage. It is a FE based method which identifies the nodes between which the damage exits. In this work DFI is formulated in the realm of WSFE. First, the cantilever beam is divided into six equal elements as shown in Fig. 9(a) and the global dynamics stiffness matrix is formed for the healthy beam. To simulate experimental condition, the time domain responses of the undamaged and damaged beams are simulated and are then used as surrogate experimental data together with the dynamic stiffness matrix of the undamaged beam to calculate the DFI. Here, the undamaged beam example used has the degraded portion of length 0.025 m at 0.25 m from fixed end of the cantilever beam of 0.75 m length, and different sizes corresponds to different values of RH. The DFI obtained are plotted for each node and for different RH in Fig. 9(b). It can be seen from the figure that the maximum peaks occur at nodes 2 and 3. Apart from this, it can observed from Fig. 9(b), that the magnitude of DFI is maximum for 80 % RH. This is in tune to the model used for simulation of response. Further, correlation can be developed between the magnitude of the DFI and extent of degradation to predict it from the DFI values. Next, knowing that the damage is in between nodes 2 and 3 from Fig. 9(a), the element between nodes 2 and 3 is again subdivided into 3 elements, to locate the position of the damage more precisely. However,

the discretization of remaining part of the beam is left same as shown in Fig. 10(a). The DFI for this new WSFE model of the beam is plotted in Fig. 10(b) for all the eight nodes as function of RH. Fig. 10(b) shows that the maximum DFI occurs at nodes 3 and 4. Thus, the degradation lies in the element between nodes 3 and 4. This is also in accordance with the simulation performed to obtain the wave response. This process of refining to predict the position of damage can be done further to obtain the exact location of damage. Thus, DFI can accurately predict the location of damage and also provide a measure of the extent of damage with very minimal computational cost.

6 Conclusions

In this paper, moisture absorbed degraded beam is modeled for wave propagation analysis and also for detection of the damage. The beam is modeled using Timoshenko beam theory with axial, transverse and rotational degrees of freedom. Here, the modeling is done using the wavelet based spectral finite element method which is especially tailored for wave propagation. The extent of degradation changes with time and relative humidity (RH) of the environment in which it is exposed. Wave based techniques are most suited to predict the presence of any small damages, because of the high frequency content of the loading. However, the effects of the minute damage/degradation on the wave responses are not visually interpretable due to minute dimension of damage. In this work, a force measure called damage force indicator has been implemented for prediction of position and location of damage from the measured wave response and dynamic stiffness matrix of the undamaged structures. The method efficiently predict the position and location of the damage. First, wave propagation in moisture absorbed degraded beam is simulated to study the effects of moisture absorption on wave propagation characteristics. Next, the simulated responses are used as surrogate experimental results to calculated the damage force indicator which gives the position and extent of damage.

References

Beylkin, G. (1992): On the representation of operators in bases of compactly supported wavelets. *SIAM Journal of Numerical Analysis*, vol. 6, no. 6, pp. 1716–1740.

Chakraborty, A.; Gopalakrishnan, S. (2004): A higher order spectral element for wave propagation analysis in functionally graded materials. *Acta Mech.*, vol. 172, pp. 17–43.

Daubechis, I. (1992): Ten lectures on wavelets. CBMS-NSF Series in Applied Mathematics, Philadelphia: SIAM.

DeIasi, R.; Whiteside, J. (1978): Effect of moisture on epoxy resins and composites. pp. 2–20. Advanced Composite Materials- Environmental Effects, ASTM, STP 658, J.R. Vinson, Ed.

Doyle, J. F. (1999): Wave propagation in structures. Springer, New York.

Han, R.; Ingber, M. S.; Schreyer, H. L. (2006): Progression of failure in fiber reinforced materials. *CMC: Computers, Materials and Continua*, vol. 4, pp. 163–176.

Han, X.; Liu, G. R.; Li, G. Y. (2004): Transient response in cross-ply laminated cylinders and its application to reconstruction of elastic constants. *CMC: Computers, Materials and Continua*, vol. 1, pp. 39–50.

Imielinska, K.; Guillaumat, L. (2004): The effect of water immersion ageing on low velocity impact behaviour of woven aramid-glass fiber/epoxy composites. *Composite Science and Technology*, vol. 64, pp. 2271–22718.

Jihua, Z.; Maosheng, Z. (2004): Visual experiments for water absorbing process of fiber-reinforced composites. *Journal of Composites Material,*, vol. 38, pp. 779–790.

Kootsooks, A.; Mouritz, A. P. (2004): Seawater durability of glass and carbon polymer composites. *Composite Science and Technology*, vol. 64, pp. 1503–1511.

Kumar, D. S.; Mahapatra, D. R.; Gopalakrishnan, S. (2004): A spectral finite element for wave propagation and structural diagnostic analysis of composite beam with transverse crack. *Finite Elemnts in Analysis and Design*, vol. 40, pp. 1729–1751.

Loos, A. C.; Springer, G. S. (1979): Moisture absorption of graphite-epoxy composites immersed in liquids and in humid air. *Journal of Composite Materials*, vol. 13, pp. 131–147.

Mitra, M.; Gopalakrishnan, S. (2005): Spectrally formulated wavelet finite elemnt for wave propogation and impactforce identification in connected 1-d waveguides. *International Journal of Solids and Structures*, vol. 42, pp. 4695–4721.

Mitra, M.; Gopalakrishnan, S. (2006): Wavelet based 2-D spectral finite element formulation for wave propagation analysis in isotropic plates. *CMES: Computer Modelling in Engineering and Sciences*, vol. 15, pp. 49–68.

Mitra, M.; Gopalakrishnan, S. (2006): Wavelet based spectral finite element for analysis of coupled wave propagation in higher order composite beams. *Composite Structures*, vol. 73, pp. 263–277.

Murthy, M. V. V. S.; Gopalakrishnan, S.; Nair, P. S. (2007): A new locking free higher order finite element formulation for composite beams. *CMC: Computers, Materials and Continua*, vol. 5, pp. 43–62.

Nag, A.; Mahapatra, D. R.; Gopalakrishnan, S. (2002): Identification of delamination in a composite beam using a damaged spectral element. *International Journal of Structural Health Monitoring*, vol. 59, pp. 105–126.

Schulz, M. J.; Naser, A. S.; Pai., P. F.; Chung, J. (1998): Locating structural damage using frequency response reference functions. *Journal of Intelligent Material Systems and Structures*, vol. 9, pp. 899–905.

Shen, C.-H.; Springer, G. S. (1976): Moisture absorption and desorption of composite materials. *Journal of Composite Materials*, vol. 10, pp. 2–20.

Smojver, I.; Soric, J. (2006): Numerical modeling of damage response of layered composite plates. *CMC: Computers, Materials and Continua*, vol. 3, pp. 13–24.

Tsai, S. W.; Hahn, H. T. (1980): Introduction to composite materials. pp. 329–376. Technomics Publishing Company, Westport, Connecticut.

Vera, A. A.; Vazquez, A. (2004): Effect of water sorption on the flexural properties of fully biodegradable composites. *Journal of Composites Material,*, vol. 38, pp. 1165–1181.

Verbis, J. T.; Tsinopoulos, S. V.; Polyzos, D. (2002): Elastic wave propagation in fiber reinforced composite materials with non-uniform distribution of fiber. *CMES: Computer Modelling in Engineering and Sciences*, vol. 3, pp. 803–814.

Whitney, J.; Browing, C. (1978): Some anomalies associated with moisture diffusion in epoxy matrix composite materials. pp. 43–60. Advanced Composite Materials- Environmental Effects, ASTM, STP 657, J.R. Vinson, Ed.

Williams, J. R.; Amaratunga, K. (1994): Introduction to wavelets in engineering. *International Journal for Numerical Methods in Engineering*, vol. 37, pp. 2365–2388.

Williams, J. R.; Amaratunga, K. (1997): A discrete wavelet transform without edge effects using wavelet extrapolation. *Journal of Fourier Analysis and Applications*, vol. 3, no. 4, pp. 435–449.